2. SHAKING TABLE TEST SETUP AND MATERIALS

A shaking table apparatus was developed in Gunsan, South Korea at Kunsan National University. The soil sample used in the test was Saemangeum dredged soil, which was obtained from an estuarine tidal flat in Gunsan city on the coast of the Yellow Sea in South Korea. The properties and the particle size distribution curve of the Saemangeum dredged soil are shown in Table 1 and Fig. 2, respectively. As shown in Fig. 2, the Saemangeum silty sand is categorized as most liquefiable soil.

Table 1. Properties of Saemangeum dredged soil

Property	Unit	Quantity
Specific gravity, G_s	NA	2.71
Percent passing #200 sieve	%	26.2
Soil classification (USCS)	NA	SM
Void ratio in loosest state, e_{max}	NA	1.37
Void ratio in densest state, e_{min}	NA	0.68
Relative density, D_r	%	50

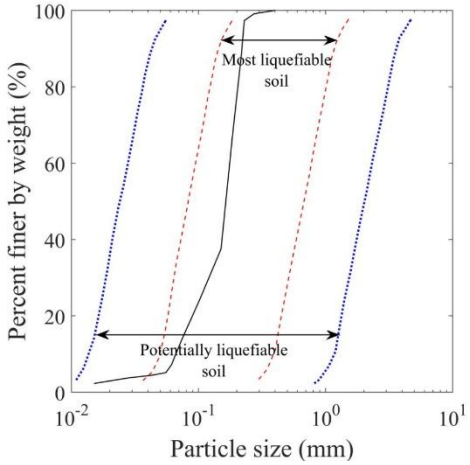

Fig. 2. Particle size distribution curve of Saemangeum dredged soil

The shaking table and scale model test setup is shown in Fig. 3. Instead of rollers, the table is supported by 12 springs to allow vertical and horizontal movements. Although, the table could move in three directions (x, y, z), transverse movement was restricted by installing cylindrical bars to achieve a plane strain condition. Glass strips were installed at the sides of the table near the location of the cylindrical bars to reduce friction between the bars and the table. For easy transportation or relocation of the apparatus, rollers or wheels were installed at the bottom of the shaking table. To secure the apparatus in place, as well as to balance or level the table, balance rods were also installed as shown, which can be adjusted by rotation to be able to increase or decrease the elevation of the table. The motion of the shaking table is powered by a DC geared motor in which the maximum frequency and horizontal motion at the base of

the table are 3 Hz and 5 cm, respectively. The speed of the motor is regulated via a speed controller while the horizontal displacement at the base can be varied by modifying the adjustable rod that connected the shaking table and the crank.

On top of the shaking table is a test tank having dimensions of 3.0 m in length, 0.7 m in height, and 0.7 m in width. At the bottom of the test tank, three translucent hoses were installed at equal space intervals to allow checking and adjustment of the water table. For easy viewing of the test specimen, the front and back of the test tank were made of transparent glass. Styrofoam with thickness of 2 cm were placed within the box at the sides to allow shear deformation of the sand during vibration. Before placing the soil sample in the tank, the inner walls were lubricated to minimize soil adhesion. A total of 11 pore water pressure gauges, 7 soil pressure gauges, and 5 accelerometers were used in the test. The sensors were placed in the manner as shown in Fig. 4 and were connected to data loggers that transmit the data readings into computers. Before placing the soil sample, vertical soil pressure gauges (SPV1) and pore pressure gauges (PP1) were placed at the bottom of the tank and horizontal soil pressure gauges (SPH1, SPH2, SPH3) were attached at the sides of the walls.

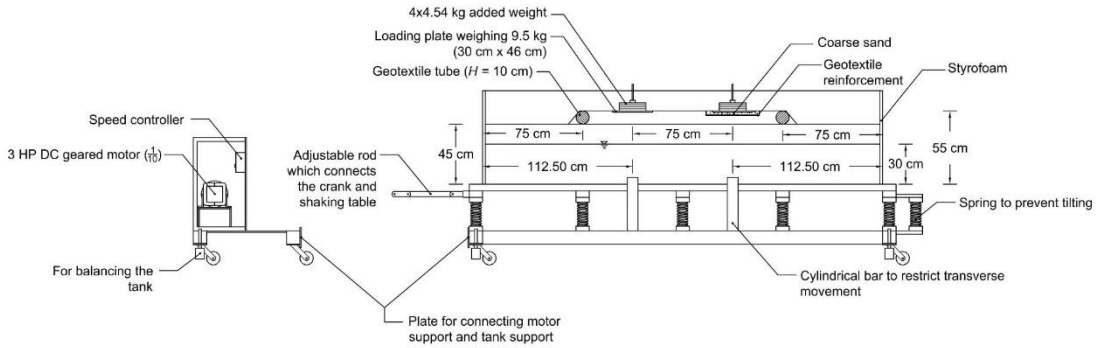

Front view

Fig. 3. Shaking table and scale model test setup

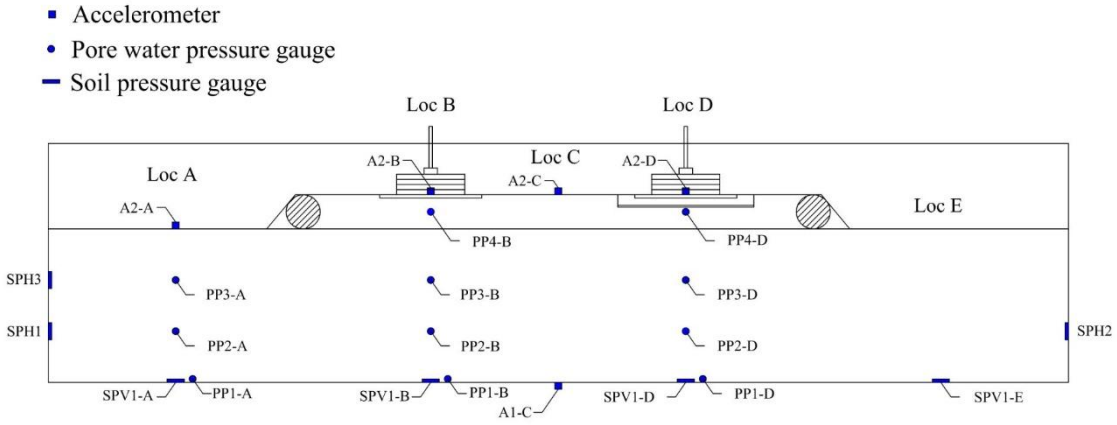

Fig. 4. Sensor locations and labels

3. RESULTS

The predominant frequency and period in the shaking test were 1.25 Hz and 0.80 s, respectively, as shown in Fig. 5. The recorded horizontal and vertical accelerations during shaking are shown in Figs. 6 and 7, respectively. The shaking table was excited in the longitudinal direction at a base motion of 0.15g, as shown in Fig. 6a. Looking at the surface accelerations (A2), sharp response accelerations occurred earlier at location A at about 180 seconds, indicating that liquefaction of the model occurred first outside of the embankment. The reason for this is that overburden pressure outside of the embankment is smaller in comparison to the soil under the embankment. Since the soil outside of the embankment started to weaken, triggering large displacements and loss of bearing capacity, the geotextile tube reinforcement was also displaced horizontally as well as vertically. Due to the rise of water outside of the embankment and due to geotextile tube displacement, water possibly migrated into embankment soil, and as a result, the shallow foundations started to settle.

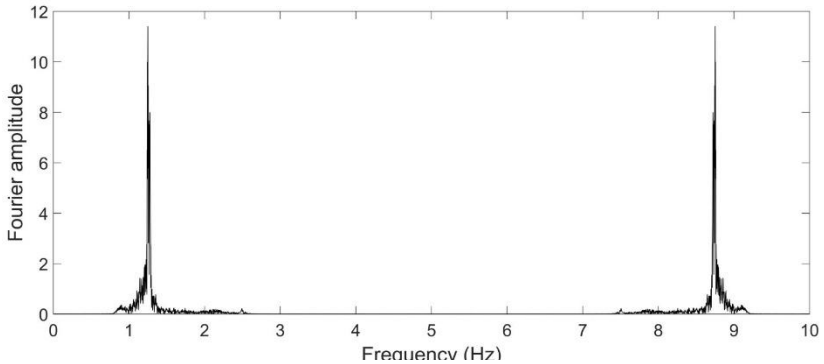

Fig. 5. Fourier spectrum showing a predominant frequency of 1.25 Hz

Sharp vertical accelerations were observed at about 190 seconds as shown in Figs. 7b and 7c. In addition, it is evident that larger foundation settlements started to occur in location B at about 190 seconds at a longer duration than at location D, wherein large foundation settlements only started occur at about 230 seconds. At the end of shaking, the foundation at location B settled to about 13 cm while the foundation at location D settled to about 10 cm. Larger horizontal accelerations were also observed in the embankment soil in comparison to the soil outside of the embankment. Furthermore, the horizontal acceleration at the surface of location C were excessively large. The reason for this is that the accelerometer was placed in the open ground, allowing it to freely move horizontally in comparison to the accelerometers in locations B and D, in which the distinct movement is in the vertical direction (settlement of the foundation). Comparing the horizontal accelerations at location B and D, large accelerations occurred at longer durations in location B than at location D. This could be due to the reinforcement and improvement of the foundation soil in location D.

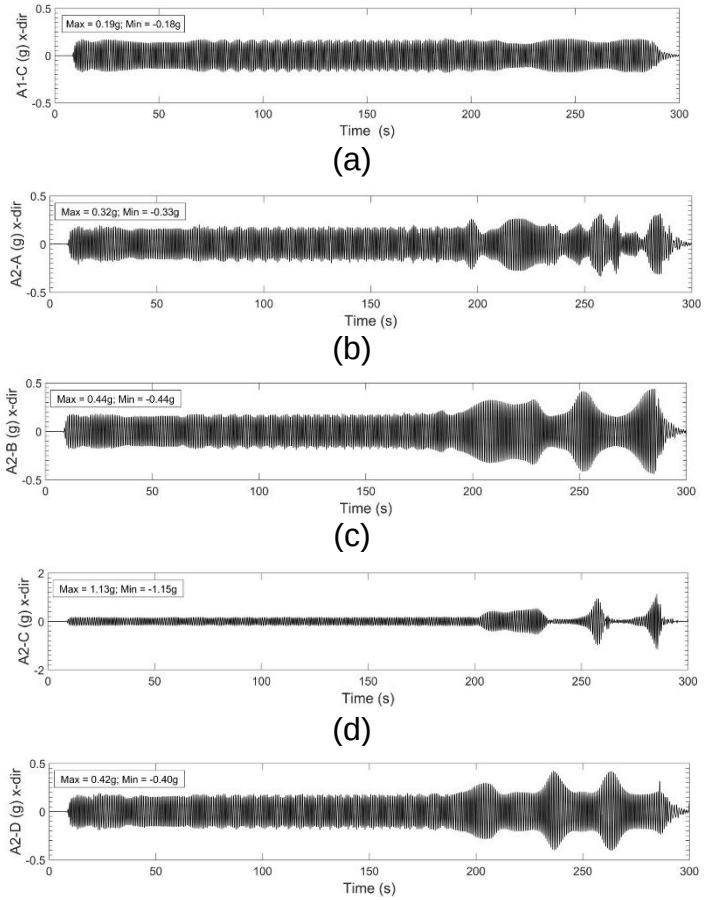

Fig. 6. Recorded horizontal accelerations: a) A1-C, b) A2-A, c) A2-B, d) A2-C, and e) A2-D

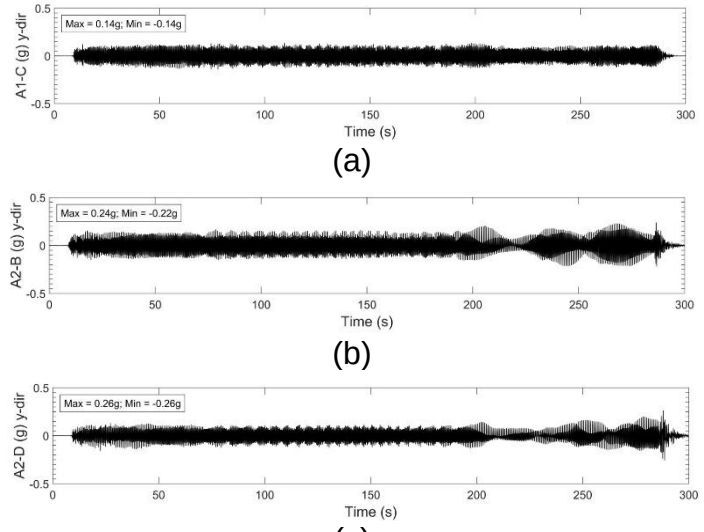

Fig. 7. Recorded vertical accelerations: a) A1-C, b) A2-B, and c) A2-D

A sample plot of the variation of shear modulus (G) with shear strain (γ) at PP3 is shown in Fig. 8. The results show that G decreases as shear strain increases. Hence, as the soil begins to liquefy, it becomes less resistant to shearing deformation. The results also show that the maximum shear modulus (G_{max}) is smallest at location A since the overburden pressure at PP3-A is smaller in comparison to the overburden pressures at PP3-B, PP3-C, and PP3-D. G_{max} at PP3-B, PP3-C, and PP3-D fall in the range of 38-48 MPa with G_{max} being the largest at PP3-D, which may be a result of the reinforcement and improvement of the foundation soil.

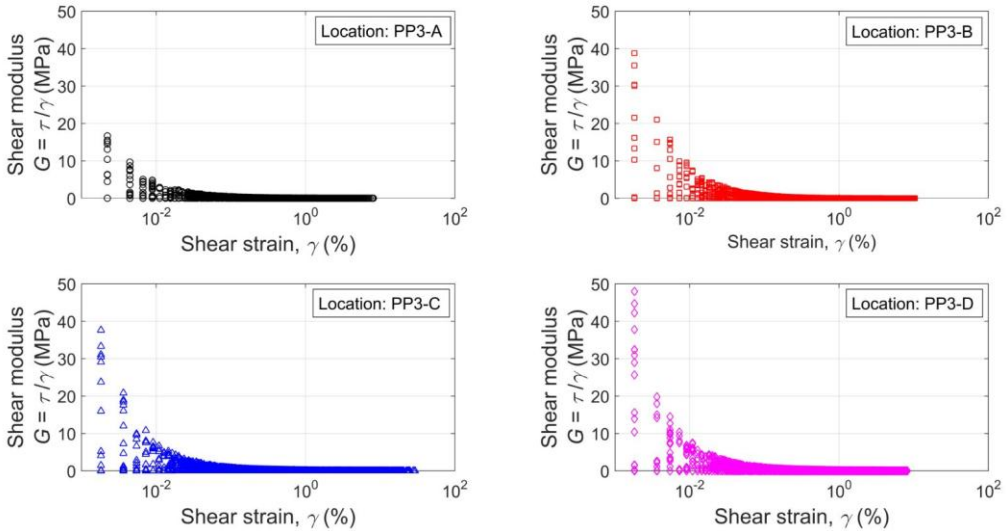

Fig. 8. Variation of shear modulus (G) with shear strain (γ) at PP3

Data readings from the pore pressure gauges at various locations are shown in Figs. 9 and 10. The excess pore water pressures at location A reached average peak values at about 165 s while at location B and D, average peak values were realized at about 180-220 s. Comparing the bottom excess pore water pressures (PP1), as shown in Fig. 10, the average peak values at locations B and D are about 1.5 times more than at location A. This is due to the fact that the height of the liquefiable soil was larger at these locations especially since the embankment was partially saturated. Similar to the readings obtained from the accelerometers, results suggest that ultimate soil weakening occurred first at location A, followed by location B, and lastly by location D. The excess pore water pressures at location A are initially larger than at locations B and D. As time elapsed, the excess pore water pressures at locations B and D started to slowly exceed location A. This is because the initial effective stress and the liquefiable height were larger at locations B and D than at location A. The increase in the excess pore water pressure outside of the embankment may have also contributed in the immediate rise of the pore water pressure inside the zone of the embankment. It can be observed at t = 200 s, the excess pore water pressure at location A exceeded the initial effective stress while the excess pore water pressure at location B was about 67% of the initial effective stress. If we look at the excess pore water pressures at PP3-

B, PP3-D, PP4-B, and PP4-D, a sudden rise in the excess pore water could be observed at about t = 180 s. This was the point in time where location A started to liquefy. Before this point in time, the rate of excess pore water pressure generation was low.

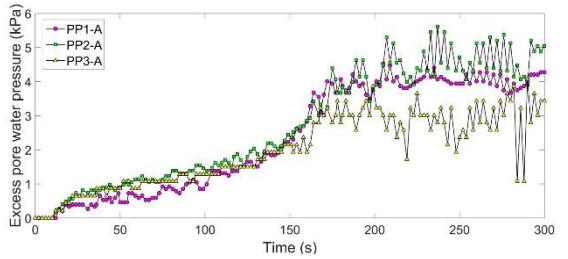

(a)

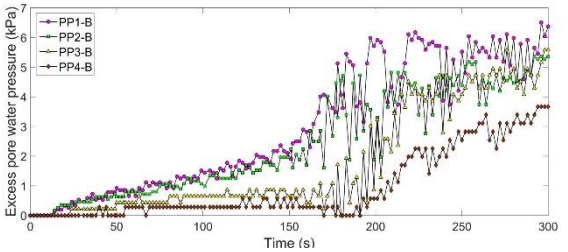

(b)

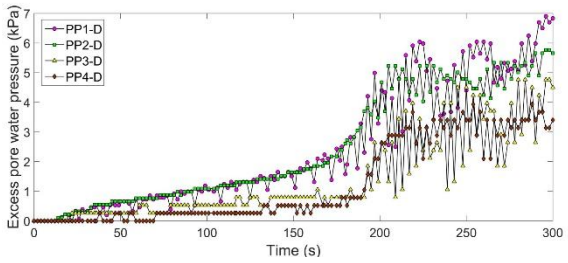

(c)

Fig. 9. Variation of excess pore water pressure at various locations: a) location A, b) location B, and c) location D

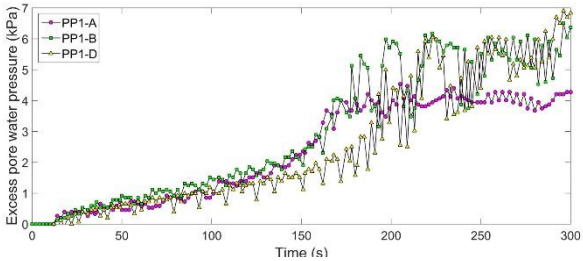

Fig. 10. Bottom excess pore water pressures

4. CONCLUSIONS

In this study, a shaking table test of a geotextile tube-reinforced embankment scale model laid on Saemangeum dredged soil, which is classified as silty sand (SM) and is most liquefiable, was conducted. The behavior of unreinforced and reinforced shallow foundations that were laid on top of the embankment were also explored. Based on the results of the experiment, the following conclusions are drawn:

- Liquefaction of the model occurred first outside of the embankment.
- Larger foundation settlements started to occur earlier in location B at a longer duration than at location D.
- The horizontal accelerations at the ground surface of the embankment were excessively large.
- Shear modulus decreases as shear strain increases or as the excess pore water pressure increases.
- The increase in the excess pore water pressure outside of the embankment may have also contributed in the immediate rise of the pore water pressure inside the zone of the embankment.

ACKNOWLEDGMENTS

This research was supported by the Korea Institute of Energy Technology Evaluation and Planning (KETEP) (No. 20183010025200) and the National Research Foundation of Korea (NRF-2017R1D1A3B03034189).

REFERENCES

Byrne, P.M. (1991), “A cyclic shear-volume coupling and pore pressure model for sand”, *Proceedings: Second International Conference on Recent Advances in Geotechnical Earthquake Engineering and Soil Dynamics*, St. Louis, Missouri.